Research Article | Vol. 26, No. 9 | 30 Apr 2018 | OPTICS EXPRESS 11850
Optics EXPRESS

High-order mode direct oscillation of few-mode fiber laser for high-quality cylindrical vector beams

TENG WANG,[1] FAN SHI,[1] YIPING HUANG,[1] JIANXIANG WEN,[1] ZHENGQIAN LUO,[2] FUFEI PANG,[1] TINGYUN WANG,[1] AND XIANGLONG ZENG[1*]

[1]*Key Lab of Specialty Fiber Optics and Optical Access Network, Joint International Research Laboratory of Specialty Fiber Optics and Advanced Communication, Shanghai Institute for Advanced Communication and Data Science, Shanghai University, Shanghai 200072, China*
[2]*Department of Electronic Engineering, School of Information Science and Engineering, Xiamen University, Xiamen 361005, China*
[*]*zenglong@shu.edu.cn*

Abstract: Generation of high-order modes with high quality is important for the application of cylindrical vector beams in fibers. We experimentally demonstrated high-order LP_{11} mode generation and amplification with a broad bandwidth in an all few-mode fiber laser. A wavelength-division-multiplexing (WDM) mode selective coupler (MSC) is proposed to achieve efficient mode conversion from LP_{01} mode to LP_{11} mode, but also combine high-order LP_{11} modes at the wavelengths of 980/1550 nm. To the best of our knowledge, this is the first report on the high-order mode oscillation in an all few-mode fiber laser. LP_{11} mode and cylindrical vector beams including radially and azimuthally polarized beams are obtained with high modal purity. The purity of the generated high-order modes are all in excess of 95%.

OCIS codes: (060.3510) Lasers, fiber; (060.2410) Fibers, erbium; (060.2320) Fiber optics amplifiers and oscillators.

References and links

1. H. Chen, C. Jin, B. Huang, N. Fontaine, R. Ryf, K. Shang, N. Grégoire, S. Morency, R. J. Essiambre, and G. Li, "Integrated cladding-pumped multicore few-mode erbium-doped fibre amplifier for space-division-multiplexed communications," Nat. Photonics **10**(8), 529–533 (2016).
2. J. V. Weerdenburg, R. Ryf, J. C. Alvarado-Zacarias, R. A. Alvarez-Aguirre, N. K. Fontaine, H. Chen, R. A. Correa, Y. Sun, L. Gruner-Nielsen, and R. Jensen, "138 Tbit/s mode- and wavelength multiplexed transmission over 6-mode graded-index fiber," J. Light. Technol. **36**(6), 1369–1374 (2018).
3. C. Xia, G. Li, N. Bai, and N. Zhao, "Space-division multiplexing: the next frontier in optical communication," Adv. Opt. Photonics **6**(4), 5041–5046 (2014).
4. D. J. Richardson, J. M. Fini, and L. E. Nelson, "Space-division multiplexing in optical fibres," Nat. Photonics **7**(5), 354–362 (2013).
5. T. Wang, F. Wang, F. Shi, F. Pang, S. Huang, T. Wang, and X. Zeng, "Generation of femtosecond optical vortex beams in all-fiber mode-locked fiber laser using mode selective coupler," J. Light. Technol. **35**(11), 2161–2166 (2017).
6. J. Zheng, A. Yang, T. Wang, N. Cao, M. Liu, F. Pang, T. Wang, and X. Zeng, "Switchable wavelength vortex beams based on polarization-dependent micro-knot resonator," Photonics Res. **6**(5), 396–402 (2018).
7. M. Rahimian, F. Bouchard, H. Al-Khazraji, E. Karimi, P. Corkum, and V. Bhardwaj, "Polarization dependent nanostructuring of silicon with femtosecond vortex pulse," APL Photonics **2**(8), 086104 (2017).
8. W. Zhang, L. Huang, K. Wei, P. Li, B. Jiang, D. Mao, F. Gao, T. Mei, G. Zhang, and J. Zhao, "High-order optical vortex generation in a few-mode fiber via cascaded acoustically driven vector mode conversion," Opt. Lett. **41**(21), 5082–5085 (2016).
9. K. Wei, W. Zhang, L. Huang, D. Mao, F. Gao, T. Mei, and J. Zhao, "Generation of cylindrical vector beams and optical vortex by two acoustically induced fiber gratings with orthogonal vibration directions," Opt. Express **25**(3), 2733–2741 (2017).
10. Y. Jiang, G. Ren, H. Li, M. Tang, W. Jin, W. Jian, and S. Jian, "Tunable orbital angular momentum generation based on two orthogonal lp modes in optical fibers," IEEE Photonics Technol. Lett. **29**(11), 901–904 (2017).
11. F. Wang, F. Shi, T. Wang, F. Pang, T. Wang, and X. Zeng, "Method of generating femtosecond cylindrical vector beams using broadband mode converter," IEEE Photonics Technol. Lett. **29**(9), 747–750 (2017).

#322677 https://doi.org/10.1364/OE.26.011850
Journal © 2018 Received 7 Feb 2018; revised 13 Apr 2018; accepted 16 Apr 2018; published 24 Apr 2018

Optics EXPRESS

12. Y. Shen, G. Ren, Y. Yang, S. Yao, Y. Wu, Y. Jiang, Y. Xu, W. Jin, B. Zhu, and S. Jian, "Switchable narrow linewidth fiber laser with LP_{11} transverse mode output," Opt. Laser Technol. **98**, 1–6 (2018).
13. Z. Zhang, Y. Cai, J. Wang, H. Wan, and L. Zhang, "Switchable dual-wavelength cylindrical vector beam generation from a passively mode-locked fiber laser based on carbon nanotubes," IEEE J. Sel. Top. Quantum Electron. **24**(3), 1–6 (2018).
14. Y. Zhou, K. Yan, R. S. Chen, C. Gu, L. X. Xu, A. T. Wang, and Q. Zhan, "Resonance efficiency enhancement for cylindrical vector fiber laser with optically induced long period grating," Appl. Phys. Lett. **110**(16), 161104 (2017).
15. A. Wang, B. Sun, C. Gu, D. Chung, G. Chen, L. Xu, and Q. Zhan, "Mode-locked all-fiber laser producing radially polarized rectangular pulses," Opt. Lett. **40**(8), 1691–1694 (2015).
16. J. Dong and K. S. Chiang, "Mode-locked fiber laser with transverse-mode selection based on a two-mode FBG," IEEE Photonics Technol. Lett. **26**(17), 1766–1769 (2014).
17. B. Sun, A. Wang, L. Xu, C. Gu, Z. Lin, H. Ming, and Q. Zhan, "Low-threshold single-wavelength all-fiber laser generating cylindrical vector beams using a few-mode fiber bragg grating," Opt. Lett. **37**(7), 464–466 (2012).
18. K. Wei, W. Zhang, L. Huang, D. Mao, F. Gao, T. Mei, and J. Zhao, "Generation of cylindrical vector beams and optical vortex by two acoustically induced fiber gratings with orthogonal vibration directions," Opt. Express **25**(3), 2733–2741 (2017).
19. D. Mao, T. Feng, W. Zhang, H. Lu, Y. Jiang, P. Li, B. Jiang, Z. Sun, and J. Zhao, "Ultrafast all-fiber based cylindrical-vector beam laser," Appl. Phys. Lett. **110**(2), 021107 (2017).
20. Y. Zhou, A. Wang, C. Gu, B. Sun, L. Xu, F. Li, D. Chung, and Q. Zhan, "Actively mode-locked all fiber laser with cylindrical vector beam output," Opt. Lett. **41**(3), 548–550 (2016).
21. L. G. Wright, D. N. Christodoulides, and F. W. Wise, "Spatiotemporal mode-locking in multimode fiber lasers," Science. **358**(6359), 94–97 (2017).
22. F. Antenucci, A. Crisanti, M. Ibáñez-Berganza, A. Marruzzo, and L. Leuzzi, "Statistical mechanics models for multimode lasers and random lasers," Philos. Mag. **96**(7-9), 704–731 (2016).
23. G. D'Aguanno and C. R. Menyuk, "Nonlinear mode coupling in whispering-gallery-mode resonators," Phys. Rev. A **93**(4), 043820 (2016).
24. M. N. Zervas and C. A. Codemard, "High power fiber lasers: A review," IEEE J. Sel. Top. Quantum Electron. **20**(5), 219–241 (2014).
25. R. Ismaeel, T. Lee, B. Oduro, Y. Jung, and G. Brambilla, "All-fiber fused directional coupler for highly efficient spatial mode conversion," Opt. Express **22**(10), 11610–11619 (2014).
26. R. Ismaeel and G. Brambilla, "Removing the directional degeneracy of LP_{11} mode in a fused-type mode selective coupler," J. Light. Technol. **34**(4), 1242–1246 (2016).
27. S. Pidishety, B. Srinivasan, and G. Brambilla, "All-fiber fused coupler for stable generation of radially and azimuthally polarized beams," IEEE Photonics Technol. Lett. **29**(1), 31–34 (2016).
28. L. Luo, S. Pu, J. Tang, X. Zeng, and M. Lahoubi, "Highly sensitive magnetic field sensor based on microfiber coupler with magnetic fluid," Appl. Phys. Lett. **106**(19), 816–5408 (2015).
29. K. J. Park, K. Y. Song, Y. K. Kim, J. H. Lee, and B. Y. Kim, "Broadband mode division multiplexer using all-fiber mode selective couplers," Opt. Express **24**(4), 3543–3549 (2016).
30. S. Li, Q. Mo, X. Hu, C. Du, and J. Wang, "Controllable all-fiber orbital angular momentum mode converter," Opt. Lett. **40**(18), 4376–4379 (2015).

1. Introduction

Mode division multiplexing (MDM) technique has been introduced and developed rapidly to enhance communication capacity, and the interest in high-order modes and their potential use in MDM systems has increased significantly [1–4]. Here, one of the most important issues in MDM system is efficient generation of high-order modes with high modal purity. On the other hand, high-order mode fiber lasers have attracted a lot of attention due to their unique properties of spatial intensity and polarization distribution, such as orbital angular momentum (OAM) beams, which are spatially structured beams with helical phase front [5–10]. Several kinds of method for the generation of high-order modes based on fiber laser have been proposed and demonstrated in recent few years [11–20]. Continuous-wave (CW) and pulsed radially and azimuthally polarized cylindrical vector beams are obtained by using mode selective coupler (MSC) [11–13], long period grating (LPG) [14], few-mode fiber bragg grating (FM-FBG) [15–17], acoustically induced fiber gratings [18], lateral offset splicing technique [19, 20] and so on. However, all of these methods to generate high-order modes are based on the mode conversion of fundamental-mode oscillation in the fiber cavity.

No matter the mode conversion is inside or outside the cavity of CW or mode-locked fiber lasers, the mode purity of generated high-order modes are greatly limited by the mode conversion

Optics EXPRESS

efficiency and bandwidth. L. G. Wright *et al.* achieve spatiotemporal mode-locking (STML) based on normal-dispersion mode-locking in space and time in multimode fiber lasers, and multiple transverse and longitudinal modes are locked to create ultrashort pulses [21]. Multimode fiber laser opens a new direction in researching nonlinear wave propagation in multimode optical fibers [22, 23]. The presence of disorder also connects multimode fibers to the field of random lasers [22]. Because multimode fiber laser can reduce nonlinear optical effect using the large mode area, it has a potential application as a platform in high average power multimode fiber laser [24].

Here we experimentally demonstrated an efficient method of high-order LP_{11} mode amplification by using a wavelength-division-multiplexing (WDM) mode selective coupler (MSC), which not only improves efficient spatial overlapping between pump and signal transverse modes in the gain medium, but also inhibits fundamental mode gain. To the best of our knowledge, this is the first report on the high-order mode oscillation in few-mode fiber (FMF) lasers. LP_{11} mode and the corresponding cylindrical vector beams including radially and azimuthally polarized beams are obtained with high modal purity.

2. Coupler fabrication and working principle

A WDM-MSC is proposed to achieve efficient mode conversion from LP_{01} mode to LP_{11} mode, but also combine high-order LP_{11} modes at the wavelength of 980/1550 nm. The schematic of 980/1550 nm WDM-MSC is shown in the inset of Fig. 1(a). The principle of the MSCs is to phase match the fundamental mode in a SMF with high-order mode in a FMF, and achieve mode conversion to high-order modes [25–27]. Various techniques of fabricating MSCs have been implemented, such as weakly fused coupler [25, 26], strongly fused coupler [28], and polished couplers [29]. In weakly fused couplers, the cross-section of the two dissimilar fibers remain unchanged, which is essential for the complete power transfer between the SMF and the FMF [25].

Using weakly fused techniques to fabricate MSCs, the propagating modes both in the SMF and the FMF are guided in silica microfibers by the silica-air interface. The mode effective indices are calculated with the different fiber diameters for step-index fiber profiles. The phase-matching curves in Fig. 1(a) show the relationship between the mode effective indices and fiber diameters. The thinner the cladding radius, the lower the mode effective index. A phase-matching point is selected to match the experimental results that the coupling region width is about 26 μm. The horizontal dotted line represents the phase-matching point chosen for LP_{11} mode coupler, which indicates that the cladding diameters of the SMF and the FMF are set to 10 μm and 16.1 μm, respectively. The corresponding mode effective index is 1.442. The diameter ratio of the SMF and the FMF is about 0.62.

Then, the commercial simulation software (Rsoft) is used to solve the modes propagating in the 980/1550 nm WDM-MSC numerically. In our simulations, the SMF and FMF cladding diameters are set to 10 μm, 16.1 μm, respectively. The cladding distance between two fibers is set to 0 μm, the coupling region length is set to 6400 μm. It is clearly seen that modal power exchanges periodically between the fundamental mode and LP_{11} mode. Figure 1(b) shows the mode power transfers in the coupling region when 980 nm LP_{01} mode in the SMF converts to LP_{11} mode in the FMF. Figure 1(c) shows the mode power exchanges when 1550 nm LP_{11} mode is launched in the FMF input port. The 980 nm and 1550 nm LP_{11} modes are expected to be multiplexed at the FMF output port. Therefore the proposed 980/1550 nm WDM-MSC can not only be used as a mode converter, but also as a wavelength division multiplexer.

Based on our simulation results, the SMF is pre-tapered to about 77.5 μm (125×0.62), then carefully aligned with the FMF and fused together using the flame brushing technique. A laser source of 980 nm is launched into the SMF input port, the output powers of SMF and FMF are detected simultaneously by a power meter. The manufacturing process can automatically stop until the split ratio of the two output ports is achieved. The final tapered diameter and the

Optics EXPRESS

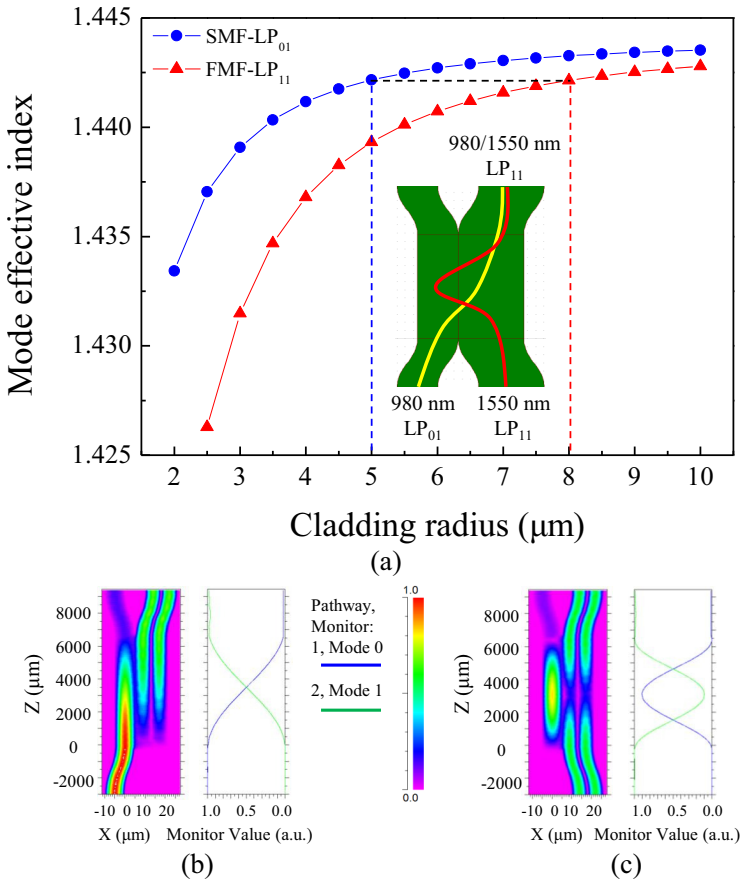

Fig. 1. (a) The mode effective index curves for the LP_{01} mode in the SMF and LP_{11} mode in the FMF versus cladding radius at the wavelength of 980 nm. The inset shows the model of the 980/1550 nm WDM-MSC in Rsoft. (b) 980 nm LP_{01} mode is launched in the SMF input port. (c) 1550 nm LP_{11} mode is launched in the FMF input port.

coupler length are obtained by optimizing the coupling efficiency in the experiment, until the power of desired LP_{11} mode in FMF is maximized. According to our experimental results, SMF is pre-tapered to diameter of 78 μm, which is agreed well with the theoretical prediction. The insertion loss of the pre-tapered SMF is measured to be smaller than 0.1 dB. The excess loss of the 980/1550 nm WDM-MSC is measured to be 0.5 dB (1.6 dB) at 980 nm (1550 nm).

To verify the 980/1550 nm WDM-MSC with a broad bandwidth, the transmission spectra of the output SMF and FMF ports are observed from 880 nm to 1080 nm by an optical spectrum analyzer (AQ6375, YOKOGAWA), as shown in Fig. 2. The mode converter has a contrast of 22 dB at the resonance wavelengths about 980 nm. It is indicated that the conversion efficiency is more than 99%. The spectrum fringes in the FMF port is caused by the interference between the degenerated vector modes of LP_{11} mode. The inset shows the mode field distribution at the FMF output port at 980 nm. The purity of the LP_{11} mode is estimated to be about 95% at 980 nm, which is measured by tight bend approach [25]. A 10-rings mode stripper with 5-mm bend radius is used to remove LP_{11} mode duo to bend loss. The power extinction ratio indicates the mode purity.

1550 nm MSC is made with the same fabrication process and working principle, but during the

Optics EXPRESS

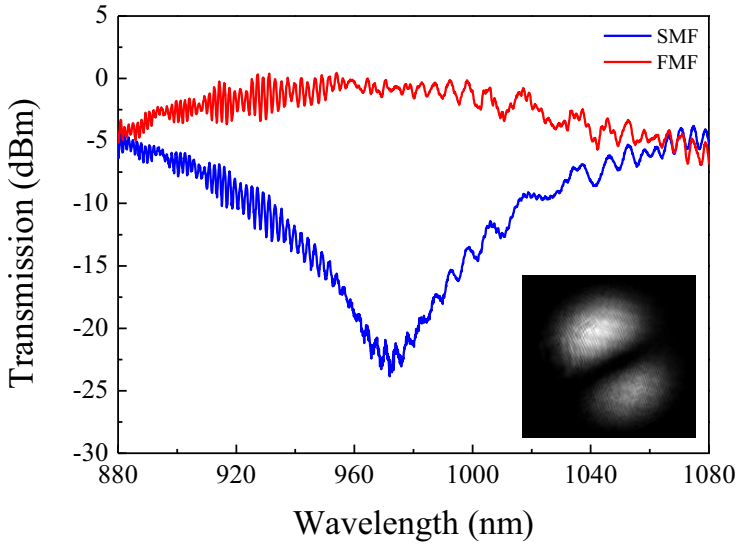

Fig. 2. Transmission spectra of 980/1550 nm WDM-MSC. The inset shows the excited 980 nm LP_{11} mode.

fabrication process, the center wavelength of light source is 1550 nm. Efficient broad bandwidth mode conversion at 1550 nm based on MSCs have been realized, which has been demonstrated in the previous work [5]. FMF-FMF coupler is made from two FMF without pre-tapering. During the fabrication process, the light source is a LP_{11} mode at the wavelength of 1550 nm. This kind of couplers can be used as a high-order mode beam splitter.

3. Experiments and discussion

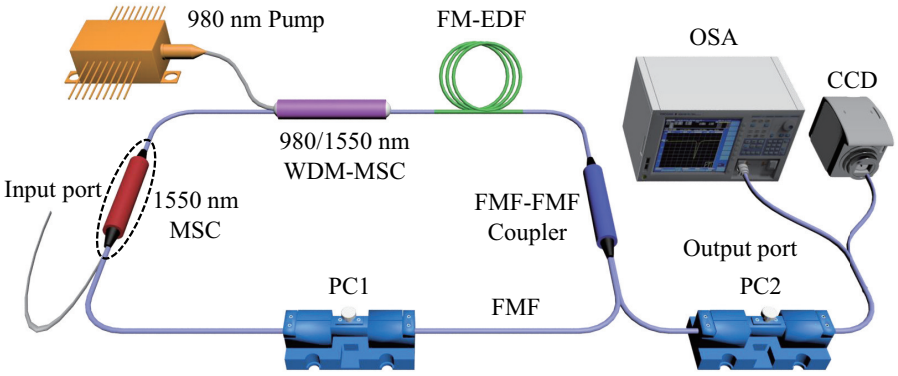

Fig. 3. Experimental setup used for LP_{11} mode oscillation in an all FMF laser. FM-EDF: few-mode erbium-doped fiber; PC: polarization controller; OSA: optical spectrum analyzer; CCD: charge coupled device, infrared camera.

The schematic of LP_{11} mode oscillation in an all-FMF laser based on WDM-MSC is shown in Fig. 3. A length of 1-m few-mode erbium-doped fiber (FM-EDF) is used as a gain medium and pumped by a 980 nm laser diode through a 980/1550 nm WDM-MSC, which not only acts as efficient mode conversion of 980 nm pump to LP_{11} mode, but also works as wavelength

Optics EXPRESS

multiplexing between LP_{11} modes at 980/1550 nm. Identical LP_{11} modes of pump and signal are crucial to generate high-order mode amplification and suppress the fundamental mode oscillation. Thus efficient mode gain are obtained through the overlap of the mode fields between signal and pump modes in the FM-EDF fiber. The output beams are recorded by using an optical spectrum analyzer (OSA) and CCD camera (InGaAs camera, Model C10633-23 from Hamamtsu Photonics).

Firstly, stimulated emission of LP_{11} mode is observed when LP_{11} mode of 980 nm pump passes through the gain medium. The use of a few-mode gain fiber provides spatial filtering and forces the laser gain to saturate with the total energy of the coupled modes [21]. A FMF-FMF coupler with power splitting ratio of 85:15 is used to extract the amplified LP_{11} mode power out of the FMF cavity.

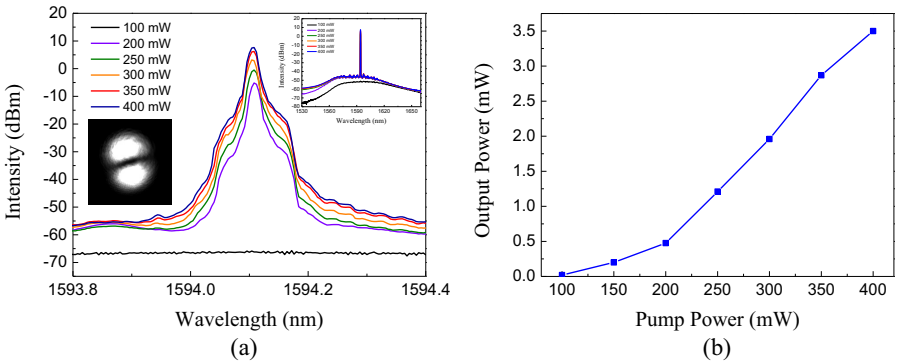

Fig. 4. (a) Optical spectra of FMF laser, the insets show the generated LP_{11} mode of FMF laser and spectra from 1530 nm to 1660 nm. (b) The relationship between pump and output powers.

LP_{11} mode oscillation at a single wavelength is analyzed as shown in Fig. 4(a). 3-dB bandwidth of the generated LP_{11} mode beam is 0.015 nm centered at 1594.1 nm. The central wavelength remains unchanged when increasing the pump power. The saturation of LP_{11} mode is also observed and another lasing at other wavelength occurs when pump power is larger than 400 mW. Figure 4(b) gives the relationship between the pump and output powers. But it is noted that without any wavelength selection applied in CW operation, the center wavelength is not stable due to the gain competition when changing the state of PC1 in the cavity.

Next, we insert another MSC at the wavelength of 1550 nm as shown in Fig. 3, which acts as a broad bandwidth mode converter. A pulsed LP_{11} signal mode is seeded into the cavity, which is generated from a mode-locking fiber laser. As shown in Figs. 5(a) and 5(b), the pulse duration is measured to be 1.78 ps with a repetition rate of 35.78 MHz and the spectral width is 25.7 nm centered at 1559 nm. The spectral width of seeded LP_{11} mode is 21.9 nm, as shown in Fig. 5(c). The input power of the seed pulse is 0.5 mW.

The gain characteristics of pulsed high-order mode based on FM-EDF are verified at different pump power as shown in Fig. 5(d). The black line represents the pulsed LP_{11} mode without 980 nm pump, the other lines represent the spectra pumped at different powers. The spectral fringes are caused by the interference between the degenerated vector modes of LP_{11} modes. Since the gain peak of FM-EDF is around 1530 nm and the amplified spectra are blue-shift when increasing the pump power. The maximum gain is about 24 dB when pump power is 400 mW. It can be seen clearly from Fig. 5(d) that the mode gain is not improved obviously with the increasing of pomp power after 200 mW duo to gain saturation.

The output spectrum is shown in Fig. 6(a) when pulsed LP_{11} mode is amplified in the FMF laser. The 3-dB bandwidth of the generated LP_{11} mode beam is 18.5 nm and its mode pattern is

Optics EXPRESS

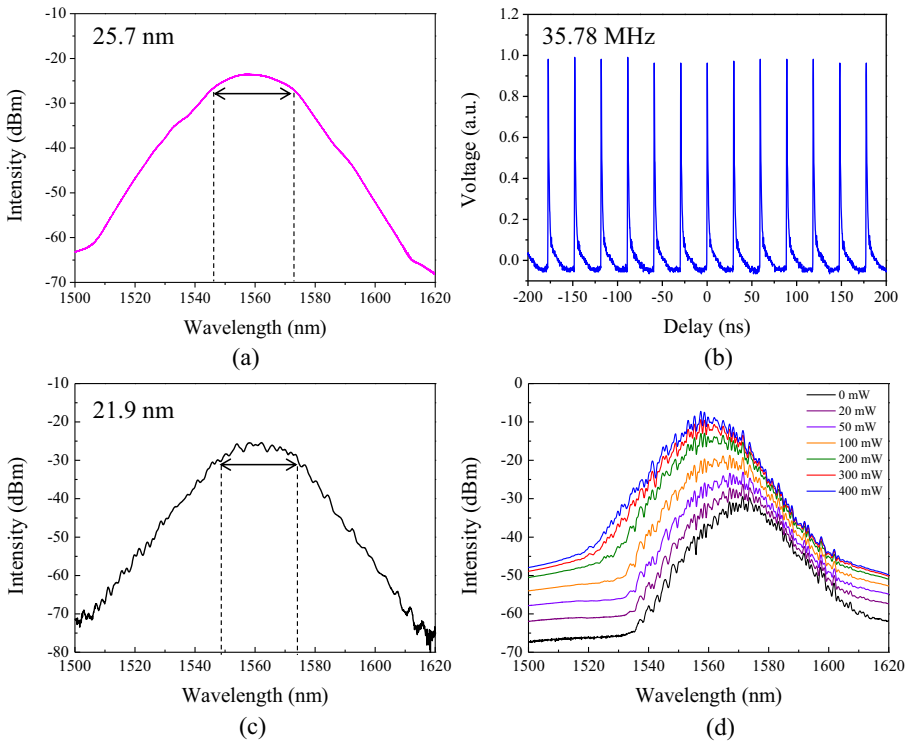

Fig. 5. (a) Optical spectrum of the LP_{01} mode pulse. (b) Mode-locked pulse trains of fiber laser. (c) Optical spectra of the LP_{11} mode pulses. (d) Gain spectra of FM-EDF at different pump power.

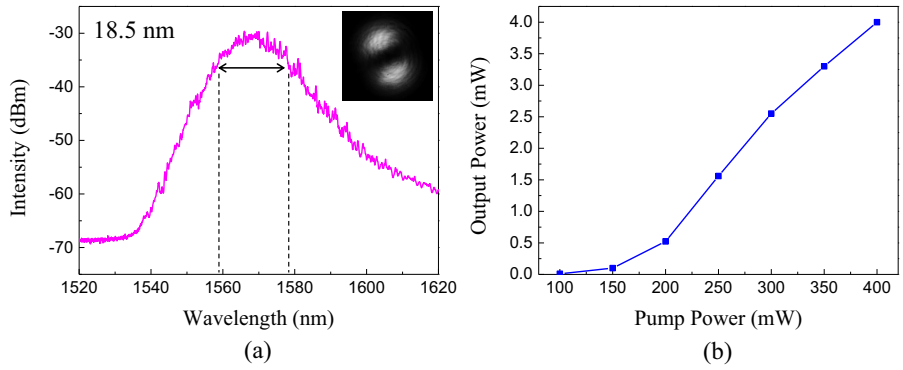

Fig. 6. (a) Spectrum of FMF laser, the inset shows the near-field pattern of the generated LP_{11} mode. (b) The relationship between pump and output powers.

Optics EXPRESS

shown in the inset. The near-field mode distribution proves LP_{11} mode with a high purity. The purity is verified in excess of 95% by tight bend approach. Figure 6(b) gives the relationship between the pump and output powers. It is noted that the output powers begin descending after 400 mW duo to the saturated gain of the signal and some CW lasing at other wavelengths. The gain of amplification in fiber laser is about 10 dB, which is smaller than that in single-pass amplifier.

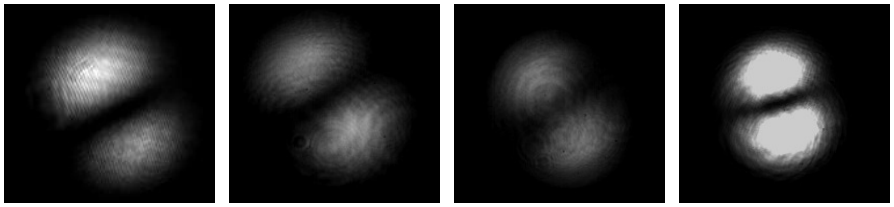

Fig. 7. Intensity distribution of LP_{11} modes in different part of FMF laser. (a) 980 nm LP_{11} mode output of 980/1550 nm WDM-MSC. (b) Pulsed LP_{11} mode output of 1550 nm mode coupler. LP_{11} mode output of FM-EDF when pump is (c) off and (d) on.

In order to further explore the high-order mode oscillation and amplification, we measure experimentally near-field patterns of LP_{11} mode in different positions of all-fiber FMF laser as shown in Fig. 7. The results show that high-order LP_{11} modes remain the same intensity patterns during mode multiplexing and amplifying process. Figure 7(a) shows the intensity distribution of output LP_{11} modes of 980/1550 nm WDM-MSC. Figure 7(b) shows the pulsed LP_{11} mode output of 1550 nm MSC. Figures 7(c) and 7(d) show the LP_{11} modes after FM-EDF when pump is off and on. It is clear that the mode of LP_{11} mode can be kept very well in the FM-EDF, and the 980 nm pump in FM-EDF is mainly in LP_{11} mode.

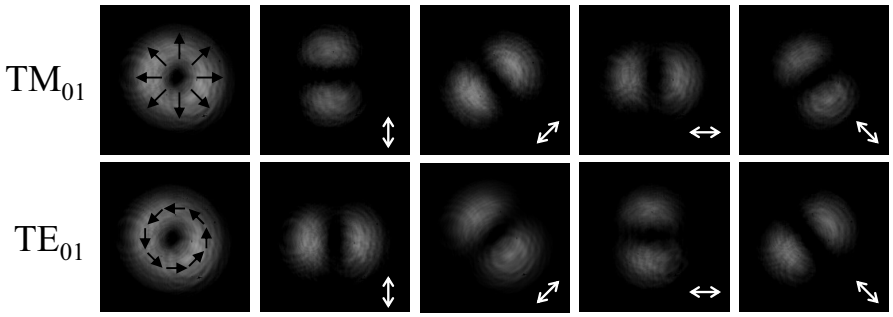

Fig. 8. Near-field intensity distribution of TM_{01} (top) and TE_{01} (bottom) modes, respectively. Two-lobe-shaped intensity patterns rotated with the polarizer. The white arrows indicate the polarizer axis.

The intensity distributions from Output port have been monitored with CCD camera, for verifying that pulsed high-order modes can always be generated. LP_{11} mode is degenerated by four vector modes possessing similar propagation constants, including TE_{01}, TM_{01}, HE_{21}^{odd} and HE_{21}^{even}. Single vector mode with different polarization state can be excited by controlling the orientations of the PC on FMF port, which refines the polarization of the output high-order modes. The degeneracy of high-order modes is removed by adjusting the PC2 based on the principle of extrusion and torsion, and the vector mode propagation constants and polarization distribution

Optics EXPRESS

could be changed [11, 30]. Using this method, donut-shaped mode patterns are obtained as shown in Fig. 8.

To testify the polarization distribution of the output beams, a polarizer is added between the FMF output port and CCD camera. Two-lobe-shaped intensity patterns are observed by rotating the polarization direction of the polarizer, which are marked with double-headed arrow indicating the transmission direction. When two-lobe-shaped intensity patterns are in the same direction as that of the polarizer, the output pulses exhibit radially polarized beam as TM_{01} mode. While the orientations of the two-lobe-shaped intensity patters are perpendicular to the polarizer, the pulses are azimuthally polarized as TE_{01} mode. The near-field mode profiles present uniform $TM_{0,1}$ and $TE_{0,1}$ mode distributions, confirming that radially and azimuthally polarized output beams with high purity are achieved. The purity of vector modes are verified by using tight bend approach [25], as well as the near-field intensity distribution is estimated to be in excess of 95%.

4. Conclusion

In conclusion, we experimentally demonstrated CW and mode-locked pulsed LP_{11} mode oscillation in an all-FMF laser for the first time, to the best of our knowledge. A novel WDM-MSC is proposed to show efficient mode conversion from LP_{01} mode to LP_{11} mode, but also combine high-order LP_{11} modes at the wavelengths of 980/1550 nm. The experimental results present that such FMF laser can be used to generate high-order mode with high modal purity. LP_{11} mode and cylindrical vector beams including radially and azimuthally polarized beams are obtained with high modal purity. The purity of the generated high-order modes are in excess of 95%. Optical vortex beams (OVBs) also can be achieved by combining different vector modes with a $\pi/2$ phase shift in the output FMF port. Efficient generation of high-order mode is supposed to be implemented by optimizing the losses of the mode couplers. Mode locking of this kind of FMF laser will be researched in the next work. The proposed approach is promising for efficiently obtaining pure vector beams in FMF lasers.

Funding

National Natural Science Foundation of China (NSFC) (91750108, 61635006, 91750115); The Program for Professor of Special Appointment (Eastern Scholar) at Shanghai Institutions of Higher Learning and Science and Technology Commission of Shanghai Municipality (16520720900); "Shuguang Program" supported by Shanghai Education Development Foundation and Shanghai Municipal Education Commission (16SG35).